Supplemental methods, figures, legends for movies, tables and references:

IFN-γ drives inflammatory bowel disease pathogenesis through VE-cadherin-directed vascular barrier disruption

Victoria Langer, Eugenia Vivi, Daniela Regensburger, Thomas H. Winkler, Maximilian J. Waldner, Timo Rath, Benjamin Schmid, Lisa Skottke, Somin Lee, Noo Li Jeon, Thomas Wohlfahrt, Viktoria Kramer, Philipp Tripal, Michael Schumann, Stephan Kersting, Claudia Handtrack, Carol I. Geppert, Karina Suchowski, Ralf H. Adams, Christoph Becker, Andreas Ramming, Elisabeth Naschberger, Nathalie Britzen-Laurent, and Michael Stürzl

Supplemental methods

Genotyping by polymerase chain reaction (PCR)

Genotyping was carried out with polymerase chain reaction (PCR) with tail genomic DNA of the mice using the following primers: Ifngr2 locus: FORWARD TGAGTTCCAAGCAAGACAGA, REVERSE CAGGGTAGAAAAGATGTGCA and INTERNAL AAGTTATGGTCTGAGCTCGC; Tie2-Cre locus: FORWARD CCCTGTGCTCAGACAGAAATGAG and REVERSE CGCATAACCAGTGAAACAGCAT and Cdh5 locus: FORWARD GCCTGCATTACCGGTCGATGCAACGA and REVERSE GTGGCAGATGGCGCGGCAACACCATT. The primers were purchased from Invitrogen (Waltham, MA, USA). PCR was performed using Red Load Taq Master high yield ready to use PCR mix (Jena Bioscience, Jena, Germany).

Flow cytometry

Single cell suspensions of spleen and thymus were prepared by gently passing the respective organ through 70 µm pore size cell strainers (Corning, New York, USA). Single

cell suspensions or blood samples were incubated with rat anti-mouse CD16/CD32 (2.5 µg/ml, catalog #: 14-0161-86, eBioscience, Waltham, MA, USA) to block non-antigen-specific binding. For membrane staining, conjugated antibodies were added for 20 min at room temperature in the dark. For intracellular staining, cells were treated with fixation/permeabilization buffer (catalog #: 00-5523-00, eBioscience), followed by incubation with conjugated antibodies in permeabilization buffer for 20 min at room temperature in the dark. Erythrocytes were lysed by using a buffered ammonium chloride (ACK) solution. Cell analysis was performed using a flow cytometer (BD LSR Fortessa, BD Biosciences, San Jose, CA, USA or CytoFLEX S, Beckman Coulter GmbH, Krefeld, Germany). Data analysis was done with FlowJo software (Tree Star, Ashland, OR, USA). Conjugated antibodies used were: rat anti-mouse CD8b (PerCP/Cy5.5, 5.3 µg/ml, catalog #: 126610, BioLegend, San Diego, CA, USA), rat anti-mouse CD3ε (Vio Blue, 13.3 µg/ml, catalog #: 130-102-203, MACS Miltenyi Biotec, Bergisch Gladbach, Germany), rat anti-mouse CD4 (eVolve 605, 5 µl/test, catalog #: 83-0042-42, eBioscience), rat anti-mouse B220 (FITC, 44.2 µg/ml, catalog #: 11-0452-82, eBioscience), rat anti-mouse CD11b (eVolve 605, 5 µl/test, catalog #: 83-0112-42, eBioscience), rat anti-mouse Ly6G (FITC, 22 µg/ml, catalog #: 11-5931-82, eBioscience), hamster anti-mouse CD11c (APC, 10.5 µg/ml, catalog #: 130-102-493, MACS Miltenyi Biotec), rat anti-mouse Ly6C (Brilliant Violet 570, 35 µg/ml, catalog #: 128030, BioLegend), rat anti-mouse F4/80 (PE, 17.5 µg/ml, catalog #: 12-4801-82, eBioscience), mouse anti-mouse CD45.1 (FITC, 1:100, catalog #: 553775, BD Biosciences), mouse anti-mouse CD45.2 (PerCP/Cy5.5, 1:800, catalog #: 45-0454-80, eBioscience), rat anti-mouse CD4 (PE, 1:800, catalog #: 553730, BD Biosciences) and rat anti-mouse CD8a (PE, 1:800, catalog #: 553033, BD Biosciences).

Isolation of mouse lung endothelial cells

Mouse lung endothelial cells were isolated using the mouse Lung Dissociation Kit from Miltenyi Biotec (catalog #: 130-095-927) according to the manufacturer's instructions. Subsequently cells were further purified by Percoll density gradient centrifugation. For

enrichment of endothelial cells, cell suspension was incubated with magnetic CD31 micro beads (Miltenyi Biotec) and magnetically enriched with a MACS Separator (Miltenyi Biotec).

RNA isolation and qRT-PCR

RNA from mouse endothelial and bone marrow cells was extracted using QIAshredder (Qiagen, Hilden, Germany) and RNeasy Mini Kit (Qiagen) according to the manufacturer's instructions. DNA digestion was performed with DNase from Ambion (Waltham, MA, USA). RNA yield was increased by glycogen precipitation. RNA quantity was determined using a Nanodrop 2000c (PeqLab, Erlangen, Germany). For qRT-PCR, Superscript III OneStep qRT-PCR Kit (Thermo Fisher Scientific, Waltham, MA, USA) was used according to the manufacturer's instructions, except for a longer reverse transcription period of 30 min at 50°C. Experiments were performed in triplicate in 96 well qPCR-plates (Agilent Technologies, Santa Clara, CA, USA) on the CFX connect (Bio-Rad, Hercules, CA, USA). As positive control commercially available reference RNA (Agilent Technologies) was used and as negative control nuclease-free water. All samples were normalized using HPRT (Hypoxanthin-Phosphoribosyl-Transferase) as a reference gene and the $\Delta\Delta$CT-method was used for further calculations. The primers and probes were purchased by Eurogentec (Lüttich, Belgium) and the following sequences were used: Ifngr2 wild-type: FORWARD CTCTTGAGCAATGTATCCTGTCACG, PROBE CAGCAAATGCCTCCGCCAGGC, REVERSE TGCCCAACGGAATCAGGATGAC; HPRT: FORWARD GGTGTTCTAGTCCTGTGGCC, PROBE TTTAGAAATGTCAGTTGCTGCGT, REVERSE CTCATAGTGCAAATCAAAAGTCTGGGG.

Western blot analysis of membrane lysates

Protein membrane lysates of MIECs were extracted by usage of Qproteome Cell Compartment Kit (Qiagen) according to the manufacturer's instructions. After separation under reducing conditions in a 10% sodium dodecyl sulfate–polyacrylamide gel and transfer onto a Roti 0.45 µm PVDF blotting membrane (Carl Roth, Karlsruhe, Germany), analysis was

performed by Western Blot as previously described (1) with the following alterations: Membranes were blocked with 3% BSA in TBS/0.1% Tween-20 for 1 h at room temperature and antibodies were diluted in 1.5% BSA in TBS/0.1% Tween-20. The following primary antibodies were used: polyclonal rabbit anti-mouse VE-cadherin (1:5,000, intercellular junction marker, catalog #: ab33168, Abcam, Cambridge, UK), monoclonal mouse anti-mouse Actin (1:2,000, catalog #: ab8226, Abcam), polyclonal rabbit anti-mouse Na,K-ATPase (1:1,000, catalog #: 3010, Cell Signaling Technology, Danvers, MA, USA). As secondary antibodies, rabbit anti-mouse (catalog #: P0260) and goat anti-rabbit (catalog #: P0448) antibodies coupled to horseradish peroxidase (each from Dako, Santa Clara, CA, USA) were used at a 1:5,000 dilution. Protein detection was performed via enhanced chemiluminescence Western blot detection system (ECL; GE Healthcare, Little Chalfont, UK) and a chemoluminescence detector (Amersham Imager 600, GE Healthcare, Chicago, IL, USA).

Immunocytochemistry

MIECs were seeded in gelatin-coated chamber slides (Falcon, Corning, New York, USA) at a density of 5×10^4 cells per cm^2. After reaching confluency, cells were treated for 48 h with either 100 U/ml mouse recombinant IFN-γ (BioLegend), 30 ng/ml mouse recombinant VEGF-A (Immunotools, Friesoythe, Germany), 0.01 µg/ml imatinib (Gleevec, Novartis) or a combination of these. Functional blockade of VE-cadherin was achieved with an anti-VE-cadherin antibody (rat anti-mouse VE-cadherin, clone BV13, 50 µg/ml, catalog #: 16-1441-85, eBioscience) and isotype control (Rat igG1 kappa isotype control, 50 µg/ml, catalog #: 16-4301-85, eBioscience).

Immunocytochemistry was performed as previously described (2). Donkey normal serum (10%, Jackson Immuno Research Laboratories, Cambridgeshire, UK) was used to block nonspecific binding sites. The following primary antibodies were used for 1 h at room temperature: rabbit anti-mouse VE-cadherin (1:400, catalog #: ab33168, Abcam), and rat anti-mouse ZO-1 (1:100, clone R46.4C, Thermo Fisher Scientific). AF488 conjugated goat

anti-rabbit (1:500, catalog #: A-11008) and AF546 conjugated goat anti-rat (1:500, catalog #: A-11081, both Thermo Fisher Scientific) were used as secondary antibodies for 45 min at room temperature. Nuclei were stained with Draq5 (1:800, catalog #: 4084, Cell Signaling Technology) and slides were mounted with fluorescence mounting medium (Dako).

Proliferation assay

C57BL/6 mouse small intestinal endothelial cells (MIECs) were seeded at a density of 2 × 10^3 cells per well in triplicate in 24-well plates (Nunc, Rochester, NY, USA) in complete growth medium (Cell Biologics, Chicago, IL). After 12 h the medium was changed to starvation medium [basal mouse endothelial cell medium (Cell Biologics) with 0.5% FCS and without growth factor supplement] for 12 h. Cells were treated with either VEGF-A (10 ng/ml, Immunotools, Friesoythe, Germany), VEGF-A + anti-VEGF-A antibody (10 ng/ml, B20-4.1.1, Genentech Inc, San Francisco, CA, USA) or VEGF-A + mouse IgG2a isotype control antibody (10 ng/ml, clone MOPC-173, catalog #: 400281, BioLegend). Treatment was repeated every second day. Total cell numbers were determined at day 5 using an automatic cell counter (Z2 Coulter Particle Count and Size Analyzer, Beckmann Coulter GmbH, Krefeld, Germany).

Microfluidic 3D angiogenesis and vasculogenesis model

A microfluidic 3D chip, as previously described (3, 4), was used to study vasculogenic formation and angiogenic remodeling of microvascular networks in vitro. HUVECs were seeded in co-culture with normal human lung fibroblasts (Lonza, Basel, Switzerland) at a concentration of 5 × 10^6 cells per ml on fibrin gel, either on one side of the central channel for an angiogenesis model or placed directly into the central channel to observe assembly of a whole vascular network in a vasculogenesis model. For the angiogenesis model, on day 2 after cell attachment, recombinant human IFN-γ (100 U/ml, Peprotech, Rocky Hill, NJ, USA) was added to the media channels for 24 h. The control group received EGM-2 only. Images were taken by a tissue culture microscope (Nikon TS100, Tokyo, Japan). For the

vasculogenesis model, IFN-γ treatment started on day 3 after cell attachment and continued for 96 h, followed by AF488 labeled mouse anti-human VE-cadherin (catalog #: 53-1449-41, eBioscience) immunostaining, as described previously (3). Images were taken by a confocal microscope (Olympus FV1000). Sprout length and thickness were analyzed using ImageJ/Fiji (5).

In vitro permeability assay

The permeability of MIEC monolayers cultured on transwell filters (0.4 µm polyester membrane, Corning, New York, USA) was analyzed by the passage of FITC-Dextran (70 kDa, Sigma-Aldrich). Inserts were hydrated for 15 min at room temperature with complete endothelial cell growth medium prior to the seeding of 80,000 cells/insert in 250 µl. Growth culture medium was added to the receiver plate well at 500 µl. Outer wells were filled with PBS to avoid evaporation. Cells were incubated for 72 h at 37°C until a monolayer was formed, followed by treatment for 48 h with either an anti-VE-cadherin antibody (rat anti-mouse VE-cadherin, clone BV13, 50 µg/ml, catalog #: 16-1441-85, eBioscience) or an isotype control antibody (Rat igG1 kappa isotype control, 50 µg/ml, catalog #: 16-4301-85, eBioscience), or by treatment with recombinant mouse IFN-γ (100 U/ml, BioLegend), imatinib (0.01 µg/ml, Gleevec, Novartis) or both in starvation medium. Untreated cells in starvation medium only were taken as controls. Subsequently, inserts were transferred into fresh receiver wells containing 500 µl of starvation medium and 150 µl FITC-Dextran diluted in starvation medium (1 mg/ml) was added to each insert and incubated for 90 min at 37°C. Then, the solution with permeated FITC-Dextran in the receiver well was mixed and transferred to a black 96-well plate (Greiner, Kremsmünster, Austria). Fluorescence was measured with a fluorescence plate reader at 485 nm excitation and 535 nm emission (Spectra Max M3, Molecular Devices, San Jose, CA, USA). Each experiment was performed in triplicate.

Confocal laser endomicroscopy

pCLE was performed using the Cellvizio system with a ColoFlex UHD probe (MaunaKea Technologies, Paris, France). Before pCLE imaging, patients intravenously received 5 ml of Fluorescein 10% as a contrast agent. The pCLE was performed at the rectosigmoid junction in all UC patients and healthy controls with a picture acquisition rate of 12 frames/s. A minimum of 1 min of pCLE video recording was obtained for each patient.

Vessel permeability was calculated as the ratio of Fluorescein-signal inside the crypt lumen over total Fluorescein-signal using the software ImageJ/Fiji (5) and was given as a percentage. Only morphologically integer crypts were used for the analysis.

Intra-vital microscopy

On day 10 of DSS-colitis (acute) or of the last cycle (chronic), Fluorescein isothiocyanate (FITC)–dextran (70 kDa, Sigma-Aldrich, St. Louis, USA) was injected intravenously (10 mg/ml, 150 µl per mouse) alone or together with Cy5-labeled lectin from *Bandeiraea simplicifolia* (100 µg/mouse in PBS, catalog #: L2380, Sigma-Aldrich) to assess vessel morphology and permeability by in vivo confocal laser microscopy (TCS SPE, Leica Microsystems, Wetzlar, Germany, equipped with LAS-LAF software). For the microscopic procedure, mice were anesthetized with Xylazine (20 mg/ml, Rompun, Bayer, 8 mg/kg per mouse)/Ketamine (100 mg/ml, Ketaset, Zoetis, Parsippany, NJ, USA, 120 mg/kg per mouse), diluted in PBS, the abdomen was opened, and the colon was cut longitudinally to visualize the mucosal vasculature. The FITC-signal was quantified (counts per pixel) using the ImageJ/Fiji software (5). Vessel permeability was calculated as the ratio of FITC-signal inside the crypt lumen over total FITC-signal and was given as a percentage, according to Haep et al. (6). Only morphologically integer crypts were used for the analysis. Afterward, mice were sacrificed, and colon tissue was removed from the cecum to the rectum, and colon length was measured.

Two-photon microscopy

In order to assess VE-cadherin distribution of the vasculature on day 10 of DSS-colitis, AF647 labeled rat anti-mouse VE-cadherin (30 µg/mouse in PBS, catalog #: 138108, BioLegend) and AF594 labeled rat anti-mouse CD31 (20 µg/mouse in PBS, catalog #: 102520, BioLegend) were injected intravenously, and mice were sacrificed after 20 min of incubation. Colon tissue was extracted and fixed in 10% buffered formalin (Sigma-Aldrich) for 24 h. The samples were then dehydrated and cleared as conducted for the light-sheet microscopy. Samples were imaged using a Zeiss LSM 880 NLO Two-photon Microscope (Zeiss, Jena, Germany) equipped with a 680–1300 nm tunable and 1040 nm fixed two-photon laser from Newport Spectra-Physics (Santa Clara, CA, USA). Two-photon images were acquired with a 20× W Plan-Apochromat objective lens (NA 1.0, Zeiss). The fluorophores were excited at 780 nm (AF594, anti-CD31) and 1200 nm (AF647, anti-VE-cadherin) and specific emission of the fluorophores was detected with non-descanned GaAsP detectors at 575–610 nm (AF594) and 650–705 nm (AF647). Image stacks of the two channels were acquired sequentially with z-planes spaced 1 µm apart. The co-localization analysis was carried out with ImageJ/Fiji (5). See Supplemental Figure 12 for the ImageJ/Fiji macro used for this analysis**.**

Light-sheet microscopy

Light-sheet microscopy was used to analyze mouse vessel permeability and colon vessel morphology. At day 10 of DSS-colitis, AF594-labeled cadaverine (100 µg/mouse in PBS, catalog #: A30678, Thermo Fisher Scientific, Waltham, MA, USA) was injected intravenously as the tracer molecule. After 10 min of incubation, Cy5-labeled lectin (100 µg/mouse in PBS, Sigma-Aldrich) was injected intravenously to visualize endothelial cells. The lectin was labeled by monoreactive N-hydroxysuccinimide ester for specific labeling of amine residues according to the manufacturer's instructions (catalog #: 43020, Lumiprobe, Hannover, Germany). After a further 10 min of incubation, mice were killed by cervical dislocation. Colon tissues were fixed in 10% buffered formalin (Sigma-Aldrich) for 24 h. Then, the samples were

dehydrated in an ascending ethanol series (3 × 70%, 2 × 95%, 2 × 100%) for 30 min each at room temperature and transferred to ethyl cinnamate (Sigma-Aldrich) for at least 2 days to achieve optical clearance (7). Samples were imaged with LaVision BioTec Ultramicroscope II (LaVision BioTec, Bielefeld, Germany) using a 2× objective lens (NA 0.5, Olympus, Tokyo, Japan). The fluorophores were excited at 561 nm (AF594, cadaverine) and 640 nm (Cy5, lectin) and specific emission of the fluorophores was detected with a sCMOS camera (Andor Neo, Belfast, Northern Ireland) between 590–650 nm (AF594) and 650–710 nm (Cy5). Image stacks of the two channels were acquired sequentially with z-planes spaced 4 µm apart. Data analysis was performed using ImageJ/Fiji (5). Vessel leakage was calculated as the ratio of cadaverine signal outside the vessels over the total cadaverine signal inside and outside the vessels. See Supplemental Figure 13 for the ImageJ/Fiji macro used for this analysis.

Supplemental figures and movies

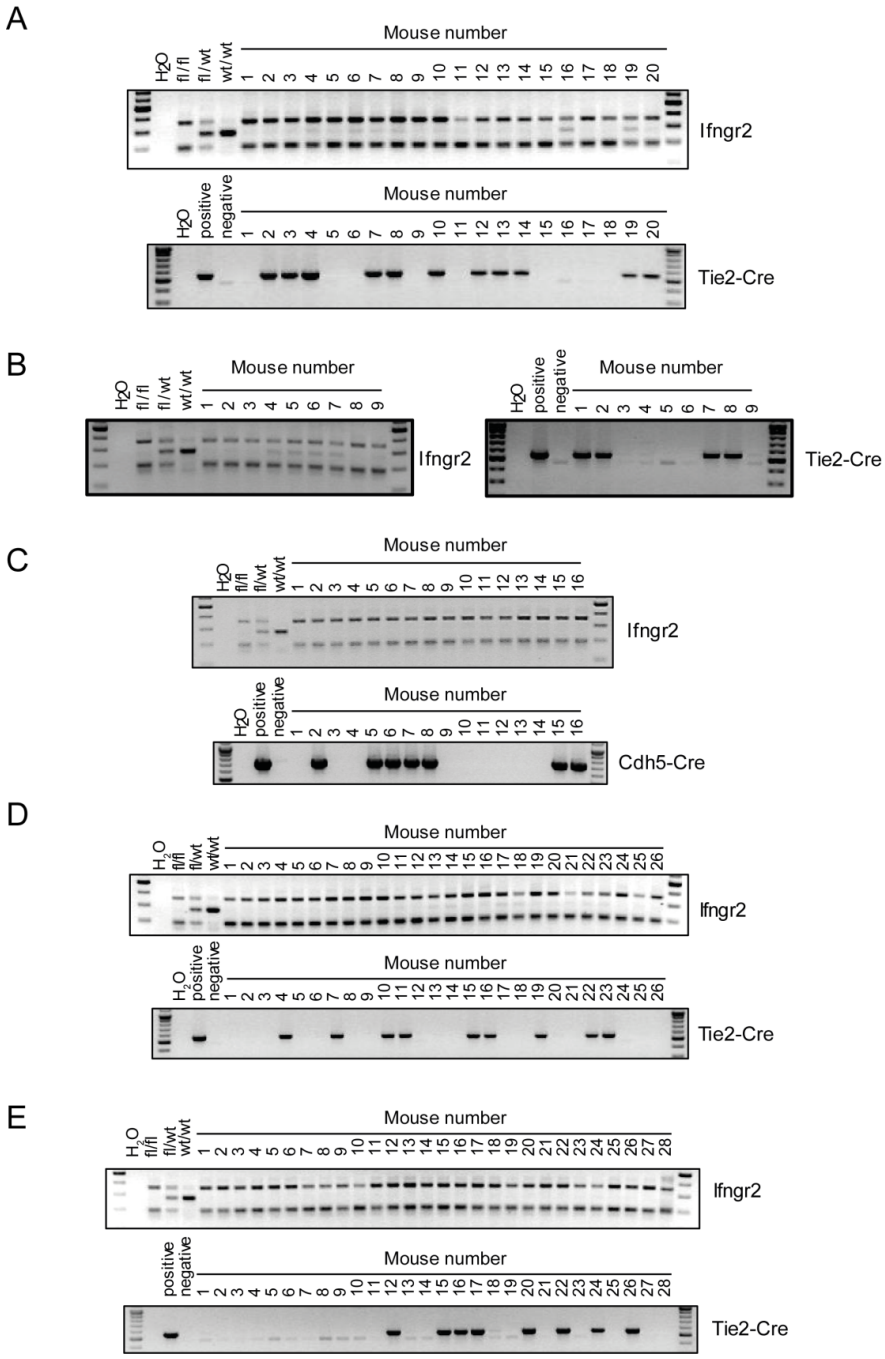

Supplemental Figure 1. Genotypic characterization of the mice included in the present study. (A-E) PCR genotyping of the Ifngr2 floxed allele and the Tie2-Cre or Cdh5-Cre transgenes was performed using tail genomic DNA for all mice included in the experiments. Genotypes of Ifngr2$^{\Delta EC}$ and control mice subjected to **(A)** acute or **(B)** chronic DSS-induced colitis, and **(C)** Ifngr2$^{i\Delta EC}$ mice subjected to acute DSS-colitis in Figure 1. **(D)** Genotypes of mice used in Figure 4 and **(E)** Figure 8. For Ifngr2, one product was obtained for the wild-type allele (wt; 275 bp) and two products for the floxed allele (fl; 191 and 357 bp). All animals included were homozygote for the floxed Ifngr2 allele. Presence of the Tie2- or Cdh-5 transgene was detected by amplification of a 600-bp or an 800-bp PCR product, respectively.

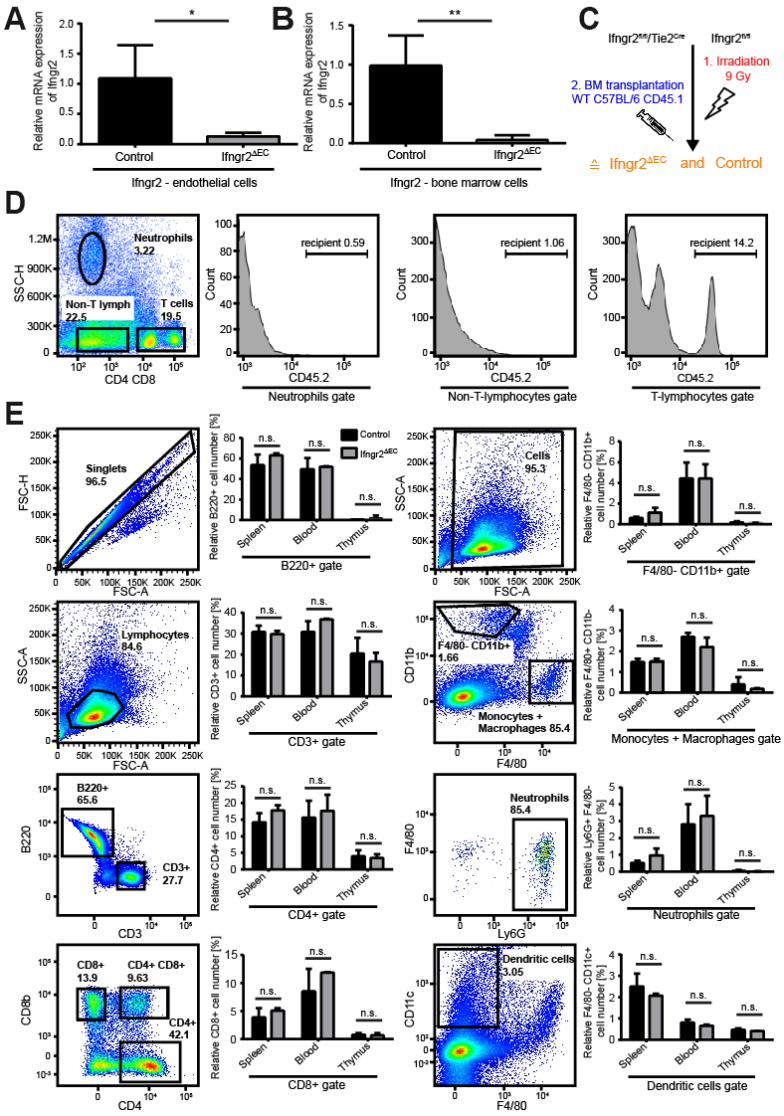

Supplemental Figure 2. Ifngr2-knockout does not affect the steady-state immune cell phenotype of mice. Ifngr2$^{\Delta EC}$ mice were generated by crossing Ifngr2$^{fl/fl}$ mice with Tie2-Cre mice. **(A, B)** Relative Ifngr2 expression as determined by RT-qPCR in isolated endothelial cells of respective mice (**A**, n = 3 each) and in bone marrow cells (**B**, n = 2 each). In contrast to control, Ifngr2$^{\Delta EC}$ mice showed a loss of receptor expression in both cell types, confirming Ifngr2 knockout. Gene expression levels were normalized to HPRT expression and are indicated as $2^{-\Delta\Delta Ct}$ values. **(C)** Schematic presentation of the generation of knockout and control mice. As Tie2 is not only expressed by endothelial cells but also by hematopoietic cells, both Ifngr2$^{fl/fl}$/Tie2^{Cre} and Ifngr2$^{fl/fl}$ mice (CD45.2 marked) underwent bone marrow transplantation with wild-type bone marrow cells (from femurs of CD45.1 marked donor mice, Pep Boy) to compensate inhibitory effects of IFN-γ receptor 2 on other than endothelial cells. Recipient mice were irradiated with 9 Gy and reconstituted with CD45.1 marked bone marrow cells. **(D)** After 6 weeks repopulation, the proportion of CD45.1 and CD45.2 cells from Ifngr2$^{\Delta EC}$ and control mice (see **C**) was analyzed from blood for T-cells (CD8+CD4+), non-T-cells and neutrophils. Representative contour blot and histograms are shown. Almost all cells were reconstituted with CD45.1+ cells. Analysis was performed for each mouse with bone marrow transplantation contributing to any of the experiments used for this study. **(E)** Flow cytometric analysis of steady-state immune cell phenotypes in control and Ifngr2$^{\Delta EC}$ mice (n = 3 each). Cells from spleen, blood and thymus were isolated and stained for B220, CD3ε, CD4, CD8b, CD11b, Ly6G, CD11c, Ly6C and F4/80. No significant differences between control and Ifngr2$^{\Delta EC}$ mice were detectable for B-cells and T-cells (CD3+, CD4+, CD8+ subtypes), monocytes and macrophages, neutrophils and dendritic cells. Representative contour plots are shown. All graphs represent means ± SD. Two-tailed, unpaired Student's *t*-test test for pairwise comparisons **(A, B)** and two-way ANOVA followed by Sidak's post-hoc test **(E)** were used to determine statistical significance (**P* < 0.05, ***P* < 0.01, n.s. = not significant).

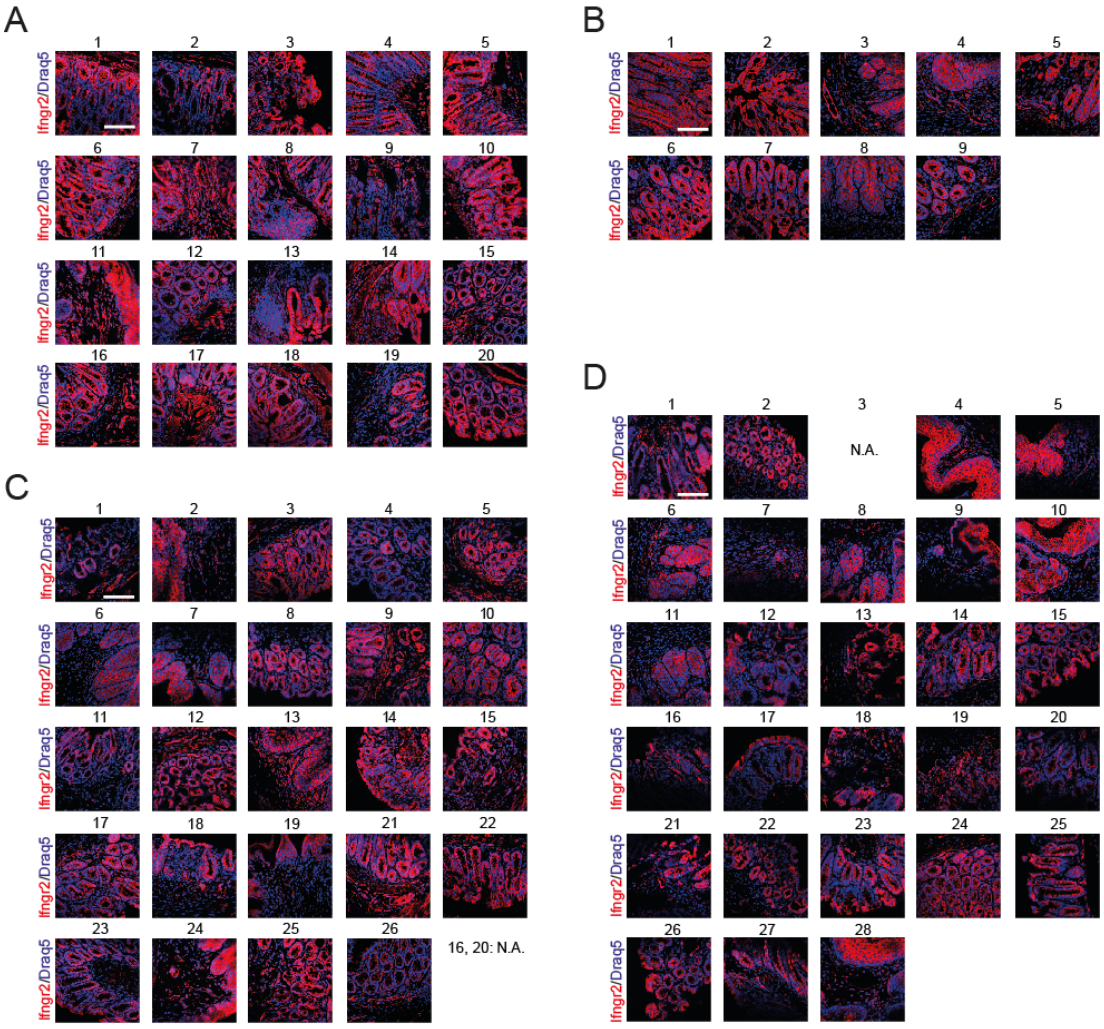

Supplemental Figure 3. Phenotypic characterization of Ifngr2$^{\Delta EC}$ and control mice subjected to acute or chronic DSS colitis. Immunofluorescence staining of murine Ifngr2 (red) in colon tissues of Ifngr2$^{\Delta EC}$ and control mice subjected to **(A, C, D)** acute or **(B)** chronic DSS-induced colitis and included in Figure 1**(A, B**), Figure 4 **(C)** and Figure 8 **(D)**. Counterstaining was performed with DRAQ5 (blue). Staining showed that the expression of the Ifngr2 in colon epithelial cells was not affected in Ifngr2$^{\Delta EC}$ and respective control mice. Scale bar: 100 µm. N.A., not available.

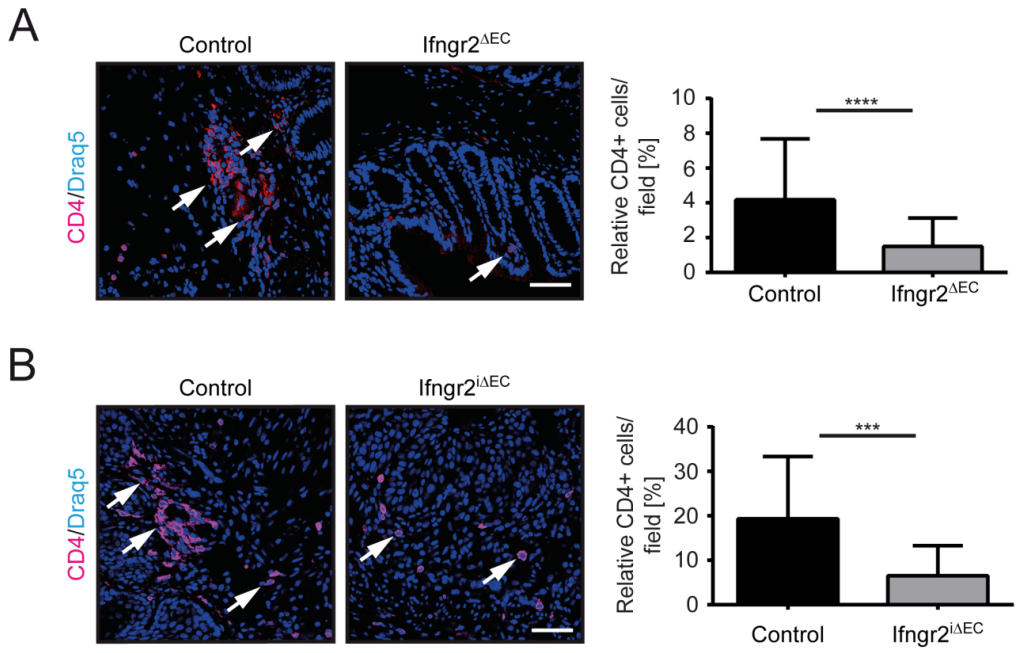

Supplemental Figure 4. Endothelial-specific inhibition of the IFN-γ response suppresses CD4+ T-cell infiltration during DSS-induced colitis in mice. Mice with **(A)** constitutive or **(B)** inducible endothelial cell-specific knockout of the IFN-γ receptor 2 ($Ifngr2^{\Delta EC}$; $Ifngr2^{i\Delta EC}$) and mice with floxed Ifngr2 alleles (Control) undergoing acute DSS-induced colitis were compared. Colonic immune cell infiltration was determined by immunofluorescence staining of CD4 (red). Nuclei were stained with DRAQ5 (blue). Arrows indicate examples for CD4 positive cells. Scale bars: 50 µm. Representative pictures are shown. Quantitative evaluations are shown on the right side of each panel, including the pooled results from two independent experiments (11 $Ifngr2^{\Delta EC}$ mice were compared with 9 control mice and 7 $Ifngr2^{i\Delta EC}$ mice with 9 control mice). All graphs represent data quantification with means ± SD. Mann-Whitney U test **(A,B)** was used to determine statistical significance (***P < 0.001, ****P < 0.0001).

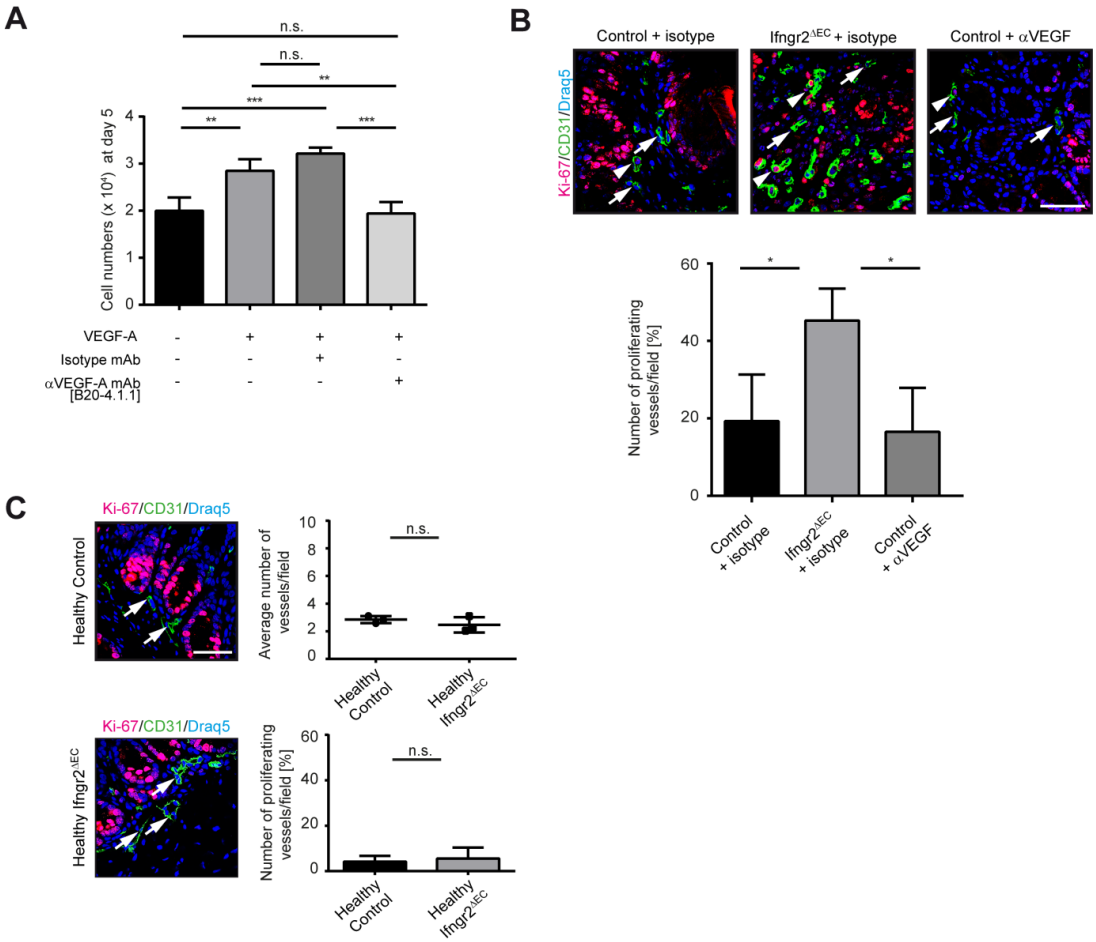

Supplemental Figure 5. Endothelial cell proliferation in DSS-colitis after treatment with the anti-VEGF B20-4.1.1 antibody or in unchallenged healthy mice. (A) MIECs treated with αVEGF-A antibody B20-4.1.1 (10 ng/ml), blocking the interaction of VEGF-A with its VEGF receptors, showed a significant inhibition of VEGF-A-induced (10 ng/ml) proliferation. IgG2a isotype control antibody (10 ng/ml) had no inhibitory effect on VEGF-A-induced proliferation. In-situ endothelial cell proliferation was evaluated **(B)** during DSS-colitis when control mice were injected with either αVEGF-A antibody B20-4.1.1 (150 µg/mouse; n = 4, 174 vessels analyzed) or with the isotype antibody (150 µg/mouse, n = 4, 196 vessels) and compared to Ifngr2$^{\Delta EC}$ mice receiving the isotype antibody (n = 4, 218 vessels), or in **(C)** unchallenged Ifngr2$^{\Delta EC}$ mice and controls. Representative images of colon tissue co-stained for CD31 (green) and Ki-67 (pink). Counterstaining was performed with DRAQ5 (blue). Scale bars: 50 µm. Arrows indicate examples of non-proliferating and arrowheads of proliferating vessels. Graphs represent means ± SD of cell numbers **(A)** numbers of vessels per field **(C, upper)** or percentage of proliferating (Ki37-positive) vessels **(B, C lower)**. One-way ANOVA followed by Tukey's post-hoc test for multiple comparisons was used for statistical evaluation in **(A and B)** and unpaired Student's *t*-test in **(C)** (*P< 0.05, ***P* < 0.01, ****P* < 0.001, n.s. = not significant.

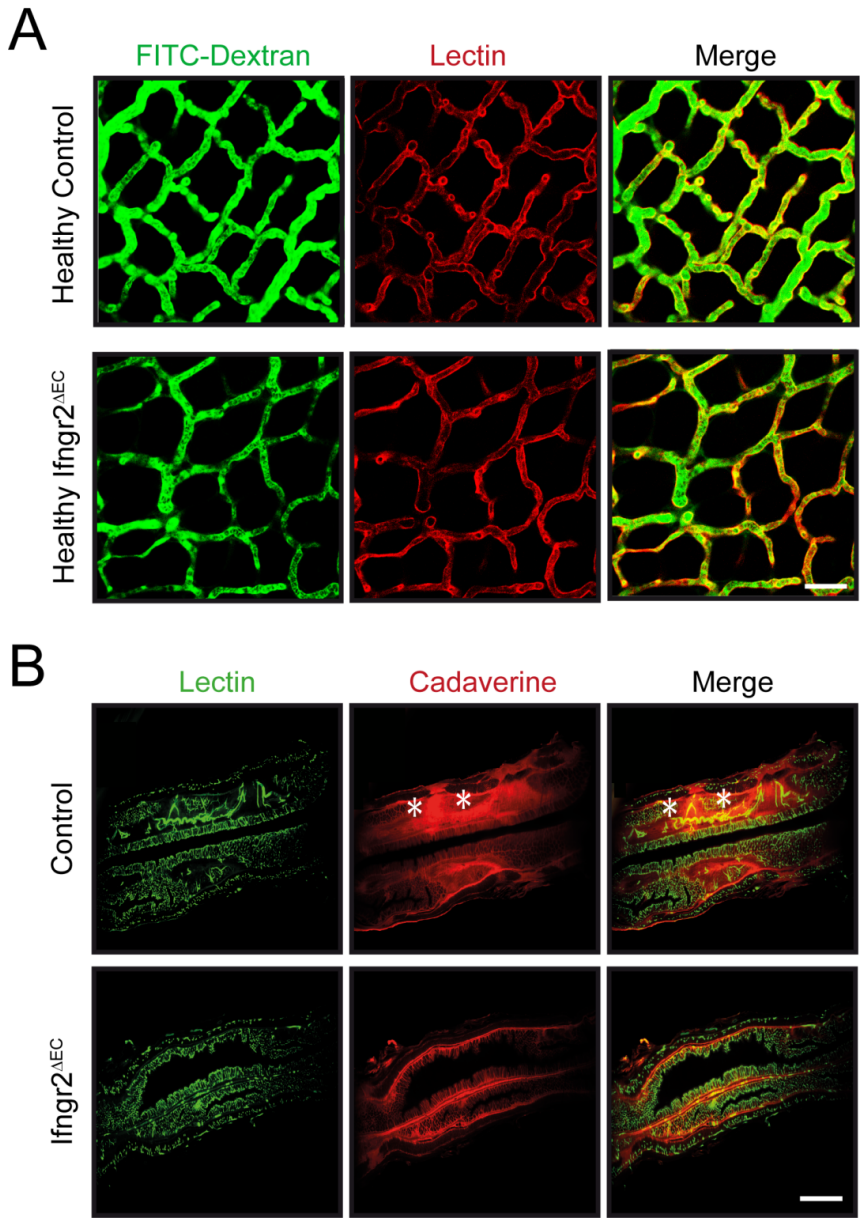

Supplemental Figure 6. Vessel permeability in unchallenged healthy and DSS-treated Ifngr2$^{\Delta EC}$ compared to control mice. (A) In vivo permeability of colonic vessels was assessed by intravenous injection of 70 kDa FITC-Dextran (10 mg/ml) and vessel structure was visualized by co-injection of Cy5-lectin (5 µg/g body weight). No vessel permeability could be detected in the colon crypts of unchallenged Ifngr2$^{\Delta EC}$ or control mice. Scale bar: 50 µm. **(B)** Colonic vessel permeability for fluorescence-labeled 0.86 kDa cadaverine (red) was visualized by light-sheet microscopy for Ifngr2$^{\Delta EC}$ and control mice with DSS-colitis (n = 3 each). Asterisks mark extravasated cadaverine. Scale bar: 500 µm.

See Supplemental Video 1

Supplemental Figure 7. IFN-γ induces vessel permeability in DSS-colitis. 3D visualization of whole colon vessels from control and Ifngr2$^{\Delta EC}$ mice with DSS-colitis by light-sheet microscopy, stained by fluorescence labeled lectin (green). Fluorescence labeled 0.86 kDa cadaverine (red) was injected intravenously. Leakage of cadaverine (marked by arrows) contributes to increased vessel permeability. Note that control mice showed increased areas of cadaverine leaking from vessels, while Ifngr2$^{\Delta EC}$ mice did not. Scale bar: 500 µm.

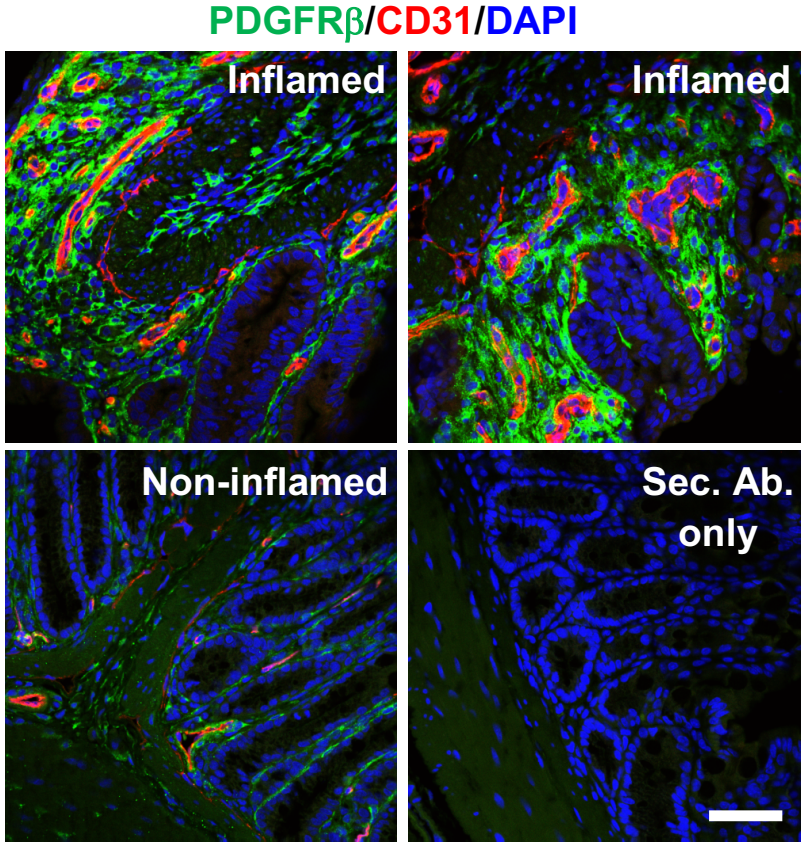

Supplemental Figure 8: Co-staining of the PDGFR-β (green), the endothelial cell-associated marker CD31 (red) and DAPI (blue) in intestinal tissues of mice with acute DSS-colitis (Ifngr2$^{\Delta EC}$ mice: n = 11; control mice: n = 9, all after bone marrow transfer). In inflamed tissues PDGFR-β expression was highly increased in many different cells as compared to non-inflamed tissues. In non-inflamed tissues PDGFR-β staining was predominantly associated with vascular structures. A control staining without the secondary antibody (Sec. Ab. only) did not show unspecific staining. Scale bar: 50 µm.

See Supplemental Video 2

Supplemental Figure 9. IFN-γ disrupts VE-cadherin junctions in DSS-colitis. 3D visualization of colonic vessels from control and Ifngr2$^{\Delta EC}$ mice with DSS-colitis by two-photon microscopy, stained by CD31 (red) and VE-cadherin (green). Control mice were marked by an irregular and tortuous vascular network with decreased VE-cadherin at endothelial cell membranes in contrast to Ifngr2$^{\Delta EC}$ mice. Scale bar: 100 µm.

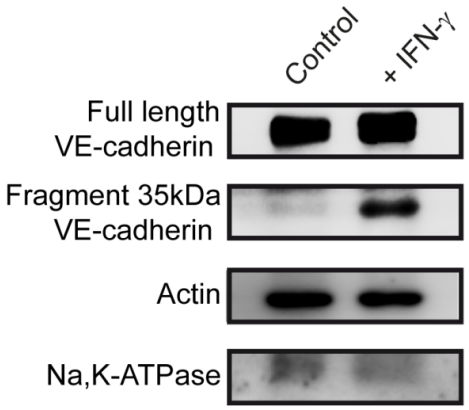

Supplemental Figure 10. IFN-γ treatment induces VE-cadherin cleavage in murine endothelial cells. Western Blot analysis of VE-cadherin expression in membrane lysates of MIECs treated with or without IFN-γ . An anti-VE-cadherin antibody recognizing the intracellular domain of VE-cadherin was used. Full-length VE-cadherin (approx. 115 kDa) was found in both untreated and IFN-γ-treated cells. An additional cleavage band was observed for IFN-γ-treated MIECs (approx. 35 kDa), suggesting an IFN-γ dependent cleavage process of VE-cadherin. Actin (approx. 42 kDa) and Na,K-ATPase (approx. 100 kDa) expression confirmed presence of membrane lysate.

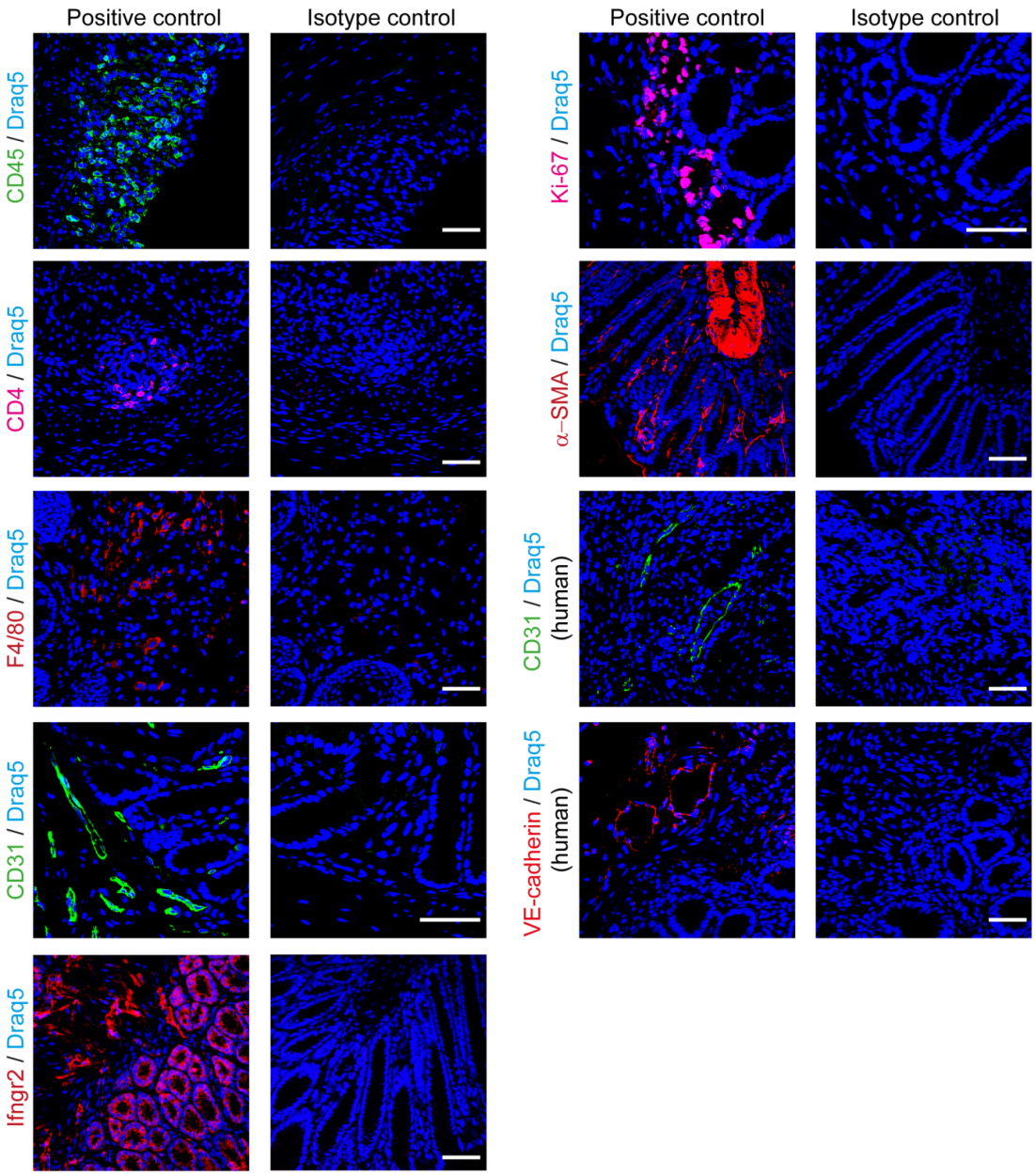

Supplemental Figure 11. Staining specificity controls of antibodies used in this study. Immunofluorescence staining of murine CD45, CD4, F4/80, CD31, Ki-67, α-SMA and Ifngr2 or human CD31 and VE-cadherin on mouse or human colon tissues, respectively. The appropriate isotype antibody for each staining was used as control to confirm specific antigen staining (Rat IgG2b, Rabbit IgG, Rat IgG2a, Rat IgG2a, Rabbit IgG, Rabbit IgG, Rabbit IgG, Mouse IgG1, Rabbit IgG, respectively). Counterstaining was performed with DRAQ5 (blue). Scale bars: 50 µm.

```
title = getTitle();

getDimensions(w, h, channels, d, frames)

rename("original");
run("Split Channels");

if(channels > 2) {
                        selectWindow("C3-original");
                        close();
}

selectWindow("C2-original");
run("Tubeness", "sigma=2.0000 use");
setAutoThreshold("Otsu dark stack");
run("Convert to Mask", "method=Otsu background=Dark black");
run("32-bit");
run("Divide...", "value=255 stack");
setMinAndMax(0, 1);

imageCalculator("Multiply create stack", "C1-original","tubeness of C2-original");
rename("inside");
selectWindow("C1-original");
getMinAndMax(min, max);
selectWindow("inside");
setMinAndMax(min, max);

selectWindow("tubeness of C2-original");
run("Invert", "stack");
imageCalculator("Multiply create stack", "C1-original","tubeness of C2-original");
rename("outside");
selectWindow("C1-original");
getMinAndMax(min, max);
selectWindow("outside");
setMinAndMax(min, max);

selectWindow("inside");
run("Subtract...", "value=300");
Stack.getStatistics(voxelCount, mean_inside, min, max, stdDev);

selectWindow("outside");
run("Subtract...", "value=300");
Stack.getStatistics(voxelCount, mean_outside, min, max, stdDev);

IJ.log("ratio inside/outside = " + (mean_inside / mean_outside));
```

Supplemental Figure 12. ImageJ/Fiji Macro used in this study. The shown macro was used in ImageJ/Fiji for analysis of in vivo co-localization of CD31/VE-cadherin (Figure 6B).

```
title = getTitle();

getDimensions(w, h, channels, d, frames)

run("Size...", "width=" + w/2 + " height=" + h/2 + " depth=" + d/2 + " constrain average interpolation=Bilinear");

rename("original");
run("Split Channels");

if(channels > 2) {
                    selectWindow("C3-original");
                    close();
}

selectWindow("C2-original");
run("Tubeness", "sigma=2.0000 use");
setAutoThreshold("Otsu dark stack");
run("Convert to Mask", "method=Otsu background=Dark black");
run("32-bit");
run("Divide...", "value=255 stack");
setMinAndMax(0, 1);

imageCalculator("Multiply create stack", "C1-original","tubeness of C2-original");
rename("inside");
selectWindow("C1-original");
getMinAndMax(min, max);
selectWindow("inside");
setMinAndMax(min, max);

selectWindow("tubeness of C2-original");
run("Invert", "stack");
imageCalculator("Multiply create stack", "C1-original","tubeness of C2-original");
rename("outside");
selectWindow("C1-original");
getMinAndMax(min, max);
selectWindow("outside");
setMinAndMax(min, max);

selectWindow("inside");
run("Subtract...", "value=300");
Stack.getStatistics(voxelCount, mean_inside, min, max, stdDev);

selectWindow("outside");
run("Subtract...", "value=300");
Stack.getStatistics(voxelCount, mean_outside, min, max, stdDev);

IJ.log("ratio outside/total = " + (mean_outside / (mean_inside + mean_outside)));
```

Supplemental Figure 13. ImageJ/Fiji Macro used in this study. The shown macro was used in ImageJ/Fiji for analysis of cadaverine leakage out of vessels (Supplemental Figure 6B).

Supplemental tables

Supplemental Table 1

Clinical characteristics of the patients included in the study of vessel permeability analysis with pCLE. Patients of the healthy control group were subjected to endoscopy to validate that unspecific abdominal pain was not due to IBD.

Patient	Sex	Age	Disease	Disease status/ Group	Location	IBD treatment	Mayo Clinical Score	Mayo Endoscopic Score	Disease duration [years]
1	m	22	Ulcerative colitis	Remission	Procto-sigmoiditis	Anti-TNFα	0	1	2
2	m	22	Ulcerative colitis	Remission	Pancolitis with Ileitis	Anti-TNFα	0	1	6
3	m	23	Ulcerative colitis	Remission	Procto-sigmoiditis	Anti-TNFα	1-2	0	21
4	f	44	Ulcerative colitis	Remission	Pancolitis with Ileitis	Anti-TNFα	1	1	21
5	f	42	Ulcerative colitis	Remission	Pancolitis	Vedolizumab	0	0-1	22
6	f	58	Ulcerative colitis	Remission	Pancolitis	Anti-TNFα	1	1	23
7	f	36	Ulcerative colitis	Remission	Procto-sigmoiditis	Anti-TNFα	0	1	4
8	m	36	Ulcerative colitis	Active disease	Pancolitis	Mesalazin	3	2	12
9	m	66	Ulcerative colitis	Active disease	Procto-sigmoiditis	Prednisolon	7	3	4
10	m	29	Ulcerative colitis	Active disease	Left-sided colitis	6-Mercaptopurin	3	2	3
11	m	20	Ulcerative colitis	Active disease	Pancolitis	Anti-TNFα	6	2	6
12	m	33	Ulcerative colitis	Active disease	Left-sided colitis	Mesalazin	2-3	2	13
13	m	47	Ulcerative colitis	Active disease	Pancolitis	Anti-TNFα Azathioprin	6	3	11
14	m	46	Ulcerative colitis	Active disease	Procto-sigmoiditis	Mesalazin	1	2	12
15	m	33	Ulcerative colitis	Active disease	Procto-sigmoiditis	Mesalazin	1-2	3	13
16	f	62	-	Healthy	-	-	-	-	0
17	f	43	-	Healthy	-	-	-	-	0
18	f	33	-	Healthy	-	-	-	-	0

Supplemental Table 2

Clinical characteristics of the patients included in the study of VE-cadherin localization in intestinal vessels. Classification of inflammation status (inflamed versus uninvolved) was based on macroscopic tissue evaluation performed by a pathologist after surgery. Relevant clinical parameters of the patients are described.

Patient	Sex	Age	Disease	Location	IBD treatment	MCS/HBI	Disease duration [years]
1	f	23	Crohn`s disease	Ileocaecal	Ustekinumab	4	9
2	f	29	Crohn`s disease	Sigmoid colon	NA	NA	11
3	f	46	Crohn`s disease	Ileocaecal; Ileoascendostomie	NA	NA	6
4	m	25	Ulcerative colitis	Colon	NA	0	4
5	m	29	Crohn`s disease	Ileocaecal	Adalimumab	2	4
6	m	22	Crohn`s disease	Ileocaecal; Ileoascendostomie	Azathioprin	2	6
7	m	23	Crohn`s disease	Jejunum; Vermiform appendix	Ustekinumab	6	5
8	f	22	Crohn`s disease	Ileocaecal; Terminal Ileum	Infliximab	1	4
9	m	36	Crohn`s disease	Ileocaecal; Ileum	Vedolizumab	NA	16
10	m	33	Crohn`s disease	Jejunum; Ileum; Sigmoid colon	NA	NA	3
11	m	60	Crohn`s disease	Sigmoid colon; Ileotransversostomy	Ustekinumab	5	45

***MCS**, Mayo Clinical Score; **HBI**, Harvey Bradshaw Index; MCS is used for ulcerative colitis and HBI for Crohn's disease; **NA**, not available.*

Supplemental references

1. Lubeseder-Martellato, C., Guenzi, E., Jörg, A., Töpolt, K., Naschberger, E., Kremmer, E., Zietz, C., Tschachler, E., Hutzler, P., Schwemmle, M., et al. 2002. Guanylate-binding protein-1 expression is selectively induced by inflammatory cytokines and is an activation marker of endothelial cells during inflammatory diseases. *Am J Pathol* 161:1749-1759.
2. Ostler, N., Britzen-Laurent, N., Liebl, A., Naschberger, E., Lochnit, G., Ostler, M., Forster, F., Kunzelmann, P., Ince, S., Supper, V., et al. 2014. Gamma interferon-induced guanylate binding protein 1 is a novel actin cytoskeleton remodeling factor. *Mol Cell Biol* 34:196-209.
3. Kim, S., Chung, M., Ahn, J., Lee, S., and Jeon, N.L. 2016. Interstitial flow regulates the angiogenic response and phenotype of endothelial cells in a 3D culture model. *Lab Chip* 16:4189-4199.
4. Kim, S., Lee, H., Chung, M., and Jeon, N.L. 2013. Engineering of functional, perfusable 3D microvascular networks on a chip. *Lab Chip* 13:1489-1500.
5. Schindelin, J., Arganda-Carreras, I., Frise, E., Kaynig, V., Longair, M., Pietzsch, T., Preibisch, S., Rueden, C., Saalfeld, S., Schmid, B., et al. 2012. Fiji: an open-source platform for biological-image analysis. *Nat Methods* 9:676-682.
6. Haep, L., Britzen-Laurent, N., Weber, T.G., Naschberger, E., Schaefer, A., Kremmer, E., Foersch, S., Vieth, M., Scheuer, W., Wirtz, S., et al. 2015. Interferon Gamma Counteracts the Angiogenic Switch and Induces Vascular Permeability in Dextran Sulfate Sodium Colitis in Mice. *Inflamm Bowel Dis* 21:2360-2371.
7. Klingberg, A., Hasenberg, A., Ludwig-Portugall, I., Medyukhina, A., Mann, L., Brenzel, A., Engel, D.R., Figge, M.T., Kurts, C., and Gunzer, M. 2017. Fully Automated Evaluation of Total Glomerular Number and Capillary Tuft Size in Nephritic Kidneys Using Lightsheet Microscopy. *J Am Soc Nephrol* 28:452-459.